J Fluoresc (2015) 25:1259–1266
DOI 10.1007/s10895-015-1614-1

ORIGINAL ARTICLE

A Indole-Trizole-Rhodamine Triad as Ratiometric Fluorescent Probe for Nanomolar-Concentration Level Hg^{2+} Sensing with High Selectivity

Heng Liu[1,3] · Hui Ding[1] · Lili Zhu[2] · Yue Wang[1] · Zili Chen[2] · Zhiyuan Tian[1]

Received: 9 June 2015 / Accepted: 30 June 2015 / Published online: 17 July 2015
© Springer Science+Business Media New York 2015

Abstract A new type of ratiometric fluorescent probe capable of detecting Hg^{2+} ions at nanomolar-concentration level with high selectivity was developed based on an indole-trizole-rhodamine triad and its practicability for intracellular Hg^{2+} sensing was verified. The as-prepared fluorescent probe is capable of detecting Hg^{2+} over other competing metal ions including Ag^{+} with high selectivity. The synergistic effect of Hg^{2+}-assisted conversion of the nonfluorescent ring-closed rhodamine moiety to the highly fluorescent ring-open form as well as the fluorescence signal amplification originating from the Förster resonance energy transfer (FRET) from indole-trizole conjugate to rhodamine moiety contributed to a detection limit of 11 nM of the probe for Hg^{2+} sensing.

Keywords Fluorescent probe · Mercury ions · Fluorescence bioimaging · Energy transfer · Recognition selectivity

✉ Yue Wang
yuewang@ucas.ac.cn

✉ Zili Chen
zilichen@ruc.edu.cn

✉ Zhiyuan Tian
zytian@ucas.ac.cn

[1] School of Chemistry & Chemical Engineering, University of Chinese Academy of Sciences (UCAS), Beijing 100049, China

[2] Department of Chemistry, Renmin University of China, Beijing 100872, China

[3] Hubei Collaborative Innovation Center for Advanced Organic Chemical Materials, Ministry of Education Key Laboratory for the Synthesis and Application of Organic Functional Molecules & College of Chemistry and Chemical Engineering, Hubei University, Wuhan 430062, People's Republic of China

Introduction

As one kind of the most toxic forms of heavy metals and widespread global pollutant, mercury is widely distributed in air, water and soil, derived from human activities such as alkali and metal processing, mining and incineration of coal, causing lethal threat to human beings [1]. The toxicity of mercury and it's other chemical forms, such as methylmercury (CH_3Hg^{+}), originates from it's highly affinity toward thiol groups of amino acids and enzymes [2]. As mercury ion can easily pass through biological membranes, long-term exposure to high levels of mercury can lead to the malfunction of cells and cause many adverse health effects in the brain, kidney, central nervous system and endocrine system [3]. The accumulation of mercury in the body can cause a series of diseases, such as Minamata disease and Alzheimer's disease [4, 5]. A considerable amount of effort has been devoted to developing new probes for detecting and analyzing mercury ion in vivo and in vitro with high sensitivity and selectivity [6–8]. Compared with conventional analytical methods such as atomic absorption/emission spectroscopy [9], plasma-mass spectroscopy [10], continuous flow cold vapor atomic fluorescence spectrometry [11], fluorescence-based detection [12–15] possesses salient figure of merits including ultrahigh sensitivity, excellent spatiotemporal resolution, facile manipulation, and suitability for high-throughput screening applications and therefore plays active roles at the forefront of bioanalysis.

In recent years, a large number of probes for mercury ion sensing were developed based on fluorescence enhancement [16–19] or quenching [20–23]. However, intensity-based fluorescent probes generally encounter some limitations, which stems from the fact that the fluorescence intensity signal is sensitive and liable to

numerous external factors including temperature, excitation power, medium characteristics, dye concentration, and detector sensitivity [24]. Ratiometric fluorescent probes are intrinsically capable of circumventing these limitations based on the built-in correlation of two fluorescence emission bands [7, 25–27]. Förster resonance energy transfer (FRET) is the most common mechanism involved in the design of ratiometric fluorescent probes. Specifically, such utility of FRET resides at the moment when fluorescent acceptor signal rises in the expense of the donor signal falls. The opposite swing of the donor and acceptor fluorescence establishes the intrinsic correlation, revealing the information of probe-analyte interactions. Rhodamine-based fluorescent probes have received tremendous attention due to their excellent spectroscopic properties such as high fluorescence quantum yield, large molar extinction coefficient, and excellent photostability. Specifically, the ring-closed rhodamine spirolactam or spirolactone derivatives typically undergo ring opening reaction, triggered by appropriate metal ions or other types of stimuli, and then converts the nonfluorescent ring-closed form of the derivatives to the counterpart ring-open spirolactam/lactone derivatives that gives rise to strong fluorescence emission [28]. Based on such conversion between spirocyclic and ring-open forms accompanied with a marked change in fluorescence emission, considerable of FRET-based fluorescent probes for various analytes have been developed [29–34]. Recently, Chen and co-workers have synthesized a novel class of indole-trizole based blue-light-emitting molecules [35]. Based on the chemical properties of trizole molecules for offering potential coordination sites for metal ions, we have reported a new type of hydrazinecarbothioamide modified trizole fluorescent probe capable of dual-channel detection of Ag^{+} and Hg^{2+} with detection limit of 97 and 142 nM, respectively [20]. In this work, we developed a new type of ratiometric fluorescent probe based on indole-trizole-rhodamine hydrazide (ITR) triad derivative for Hg^{2+} ion sensing. Specifically, such type of probe typically underwent Hg^{2+}-dependent FRET from the indole-trizole conjugate, the donor, to the rhodamine hydrazide moiety, the acceptor, and thus enabled the built-in correlation between two fluorescence emission bands sensitive to the concentration of Hg^{2+}. It is noted that Ag^{+} and Hg^{2+} are two kinds of chemically closely related heavy transition metal ions and most fluorescent probes developed to date display nonspecific fluorescence quenching upon complexation with them, which is a crucial impediment to discrimination between these two toxic metal ions [36–39]. The Hg^{2+} probe developed in this work is capable of detecting Hg^{2+} over other reference metal ions including Ag^{+} with detection limit down to 11 nM, filling the bill for the upper limit of 2 ppb (10 nM) for Hg(II) in safe drinking water that the Environmental Protection Agency (EPA) in USA set. Additionally, the preliminary cell imaging verified the practicability of this type of probes for intracellular Hg^{2+} sensing.

Experimental

Chemicals

$HgCl_2$ and other metal ion inorganic salt used in the experiments were obtained from Shanghai Shenbo Chemical Co., Ltd., China. Rhodamine B, hydrazine hydrate, 1-methyl-1*H*-indole, 1*H*-benzo[*d*][1,2,3] triazole, NIS(*N*-iodosuccinimide), *N*,*N*-dim ethylformamide (DMF), hydrazinecarbothioamide, ethanol and other organic reagents were purchased from Aladdin Chemistry Co., Ltd., China and used directly without further purification unless otherwise stated. All solutions were freshly prepared before use. Milli-Q ultrapure water (18.2 MΩcm) was used in all experiments.

Characterization

^{1}H NMR spectra were recorded in DMSO-d_6 using a Bruker 400 MHz NMR Spectrometer. UV–Vis absorption spectra were recorded on Shimadzu UV2550 UV–VIS Spectrophotometers. Fluorescence spectra were obtained on Horiba FluoroMax4 spectrofluometer. MALDI-TOF mass spectrum was performed on Bruker Biflex III MALDI-TOF spectrometer.

Synthesis

The synthetic procedure of the target fluorescence probe (ITR) is shown in Scheme 1. Rhodamine hydrazide 2 and 2-(2H-benzo[d,1,2,3]triazol-2-yl)-1-methyl -1H-indole-3-carbaldehyde was prepared according to the previously reported procedures [20, 40]. In a typical protocol for synthesis of ITR, a solution of Rhodamine hydrazide 2 (28 mg, 0.06 mmol) and 2-(2H-benzo[d,1,2,3]triazol-2-yl)-1-methyl-1H- indole-3-carbaldehyde (18 mg, 0.06 mmol) in ethanol (3 mL) was refluxed for 10 h under argon atmosphere. After the solution was cooled, the solvent was removed under reduced pressure.

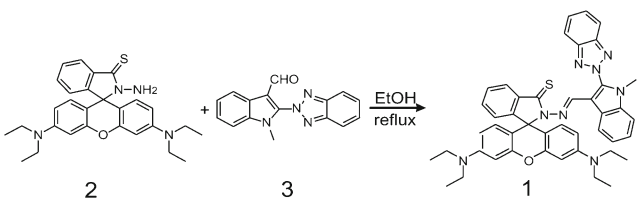

Scheme 1 Synthesis of the target indole-trizole-rhodamine hydrazide (ITR) triad fluorescent probe

The crude product was purified by column chromatography with petroleum-ethyl acetate (v/v=10/1), yielding a yellow solid *1* (27 mg, 60 %). ^{1}H NMR (400 MHz, DMSO-d_6): δ 8.79 (s, 1H), 8.38 (d, J=7.1 Hz, 1H), 8.39–7.99 (m, 4H), 7.74–7.65 (m, 4H), 7.48–7.34 (m, 4H), 7.03 (d, J=6.9 Hz, 1H), 6.62 (d, J=8.3 Hz, 1H), 6.37–6.27 (m, 4H), 3.90 (s, 3H), 3.30–3.29 (m, 8H), 1.15–0.99 (m, 12H); ^{13}C NMR (100 MHz, DMSO-d_6): δ 153.2, 151.2, 147.8, 144.9, 134.4, 131.5, 129.9, 128.6, 118.5, 109.7, 108.4, 96.8, 62.3, 43.7, 31.3, 12.4; MALDI-TOF MS: $[M-H]^-$ Calcd for $C_{44}H_{42}N_8OS$: 730.3; Found: 729.5.

Results and Discussion

The ion recognition behaviors of the as-prepared probe ITR in EtOH-MOPS mixed solvent with 70 % MOPS (v/v) were investigated using UV–Vis absorption and fluorescence emission spectroscopy. It can be clearly seen from Fig. 1a that among a series of physiologically important metal ions including Hg^{2+}, Ag^{+}, Al^{3+}, Cd^{2+}, Co^{2+}, Cr^{3+}, Cu^{2+}, Fe^{2+}, Fe^{3+}, K^{+}, Li^{+}, Mg^{2+}, Na^{+}, Ni^{2+}, Pb^{2+}, Zn^{2+}, only Hg^{2+} induced marked increase in the absorption band centered at ~565 nm while the absorption features of the probe remained nearly unperturbed upon the addition of other metal ions, suggesting the excellent ion selectivity of the as-prepared probe. Such Hg^{2+}-induced change in the absorption feature was accompnied by a clear change in the color of the probe solution from colorless to vivid pink upon addition of Hg^{2+}, as shown in the inset in Fig. 1a, suggesting the practicability of this type of probes for facile visual detection of Hg^{2+} by human eyes. The superior high ion selectivity of ITR toward Hg^{2+} was clearly demonstrated in the fluorescence emission features of the probe in the absence and presence of Hg^{2+} and other reference metal ions, as shown in Fig. 1b. It can be seen that upon addition of the reference metal ions, including Al^{3+}, Cd^{2+}, Co^{2+}, Cr^{3+}, Cu^{2+}, Fe^{2+}, Fe^{3+}, K^{+}, Li^{+}, Mg^{2+}, Na^{+}, Ni^{2+}, Pb^{2+}, and Zn^{2+}, fluorescence emission intensities of the probe solution sample centered at ~590 nm remained nearly unchanged as compared to that of the free probe. The addition of Ag^{+} induced slight increase in the emission intensity in the identical condition. In sharp contrast, a remarkable enhancement in the emission intensity of the probe solution sample was observed upon addition of five equiv. of Hg^{2+}, unequivocally indicating an excellent selectivity of ITR for Hg^{2+} over other interfering metal ions. Owing to such significant change in the fluorescence feature of the sample that Hg^{2+}-induced, a vivid yellow fluorescence color, in sharp contrast to the free probe sample, was observed.

Another noteworthy feature demonstrated in Fig. 1b is the Hg^{2+}-induced remarkable increase in the emission band centered at 590 nm concomitant with a slight decrease in the emission band centered ~490 nm. It is known that the ring-open rhodamine derivative generally possesses high fluorescence quantun yield while the counterpart spirocyclic derivative of rhodamine is nearly nonfluorescent. Taking this, it is plausible that the abovementioned remarkable increase in the emission band centered at 590 nm originated from the Hg^{2+}-induced ring-opening reaction of the probe. Additionally, the excitation wavelength of 390 nm matches the optimum absorption band of the indole-trizole conjugate, at which wavelength, however, the ring-open rhodamine derivative displays negligible absorption. Taking this, along with the increase in the emission band centered at ~590 nm at the expense of the emission band centered ~490 nm, an energy transfer process from the indole-trizole conjugate to the ring-open rhodamine moiety, as a product of the Hg^{2+} induced ring-opening reaction, was most probably involved in. Figure 2 illustrated the ratios of the fluorescence intensity at 590 nm over that at 490 nm (I_{590}/I_{490}) of the probe sample in EtOH-MOPS mixed solvent with 70 % MOPS (v/v) upon addition of various metal ions. It can be clearly seen that upon addition of the reference metal ions such as Al^{3+}, Cd^{2+}, Co^{2+}, Cr^{3+}, Cu^{2+}, Fe^{2+}, Fe^{3+}, K^{+}, Li^{+}, Mg^{2+}, Na^{+}, Ni^{2+}, Pb^{2+}, Zn^{2+}, the ratio of I_{590}/I_{490} nearly remained either unchanged or minimally affected compared to the that of ITR sample prior to the addition of metal ions. An exception case is Ag^{+}, which induced a ratio of I_{590}/I_{490} about three times that of the free probe sample. In sharp contrast to the effects that these reference metal ions exerted on the emission features of the probe sample, Hg^{2+} induced a

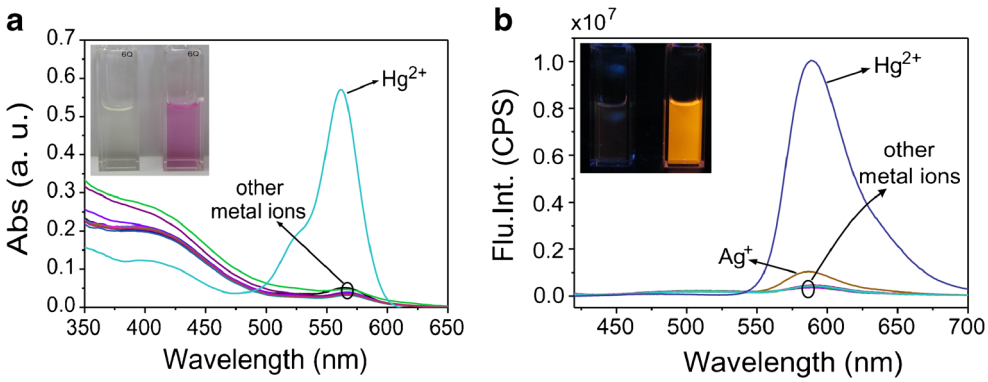

Fig. 1 UV-Visible absorption spectra (**a**) and fluorescence emission spectra (λ_{ex}=390 nm) (**b**) of probe (10 μM) in the presence of 5 equiv. of different metal ions in EtOH-MOPS mixed solvent with 70 % MOPS

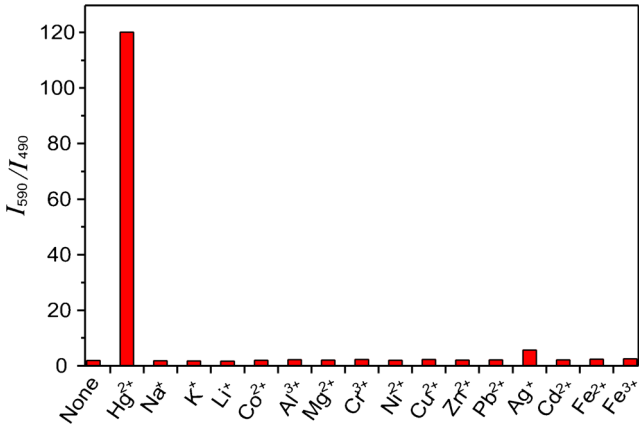

Fig. 2 Fluorescence intensity ratio (I_{590} /I_{490}) (λ_{ex}=390 nm) of probe (10 μM) in EtOH-MOPS mixed solvent with 70 % MOPS in the absence and presence of 5 equiv. of different metal ions

I_{590}/I_{490} ratio up to 120, approximately 65 times larger as compared to the free probe sample, indicating a high selectivity and sensitivity of the FRET-based probe for Hg^{2+} sensing in aqueous milieau.

In order to gain detailed information of the Hg^{2+}-probe interaction, UV–Vis absorption and fluorescence titration experiments were preformed. Figure 3a showed the changes in UV–Vis absorbance spectra of the probe in the EtOH-MOPS mixed solvent upon gradual addition of Hg^{2+}. It can be seen that upon addition of Hg^{2+}, the low-energy band with wavelength the region of 485–600 nm gradually increased at the expense of the broad characteristic absorption features in the region of 350–485 nm, resulting in a typical isobestic point at ~485 nm. Such emergence of isosbestic point and the low-energy absorption band upon addition of Hg^{2+} are indicative of a Hg^{2+}-trigered one-to-one converstion and the formation of Hg^{2+}-IRT complex. Figure 2b displayed the evolution of fluorescence emission features of the probe upon gradual addition of the probe. It can be seen that upon excitation at 390 nm, the probe displayed two weak emission bands, centered at ~490 and ~590 nm, respectively, which can be attributed to the emission of indole-trizole and ring-closed form of rhodamine hydrazide. Upon addition of Hg^{2+}, the emission band attributed to the ring-open rhodamine derivative significantly increased concomitant with a gradual decrease in the emission band of indole-trizole conjugate moiety. Informatively, such evolution of fluorescence emission spectra revealed an isosbestic-like point at ~547 nm, suggesting a Hg^{2+}-induced clean one-to-one conversion from the probe. Upon addition of 1.6 equiv. of Hg^{2+}, the fluorescence intensity of the probe sample centered at ~590 nm was almost saturated, resulting in a I_{590}/I_{490} ratio approximately 65 times larger than the counterpart ratio of the probe sample prior to the addition of Hg^{2+}. The inset in Fig. 2b displayed a plot of I_{590}/I_{490} against the concentration of Hg^{2+} ranging from 4 to 14 μM and the corresponding linear fit (R^2=0.983). Based on such titration result, a detection limit of 11 nM of the as-prepared ITR probe for Hg^{2+} sensing was obtained, which is capable of reliably sensing the Hg^{2+} concentration in drinking water with respect to the U. S. EPA limit. It is noted that our previous fluorescent probe based on the thiosemicarbazide-functionalized indole-trizole conjugate for Hg^{2+} sensing displayed a detection limit of 142 nM, which is more than one order of magnitude higher than the detection limit that the ITR probe enabled. As aforementioned, the ring-open rhodamine derivative has efficient quantum yield while the counterpart spirocyclic derivative of rhodamine is nearly nonfluorescent, which is expected to give rise to huge contrast in the fluorescence signal intensity between the cases in the absence and presence of Hg^{2+} that is capable of triggering the ring-opening reaction of the ring-closed rhodamine moiety. Additionally, as compared to the ring-open rhodamine derivative, the indole-trizole conjugate moiety displays insufficient quantum yield, typically less 0.1 [20]. Thus, the FRET process from the indole-trizole conjugate moiety to the ring-open rhodamine derivative actually enabled the amplification of the fluorescence signal for sensing. The synergistic effect of the abovementioned two factors is expected to mainly contribute to the observed disparity in the detection limits of these two types of probes.

Competetive binding experiments of Hg^{2+} with the probe in the presence of other reference metal ions with much higher concentration were performed to verify the recognition specificity of the IRT probe for Hg^{2+}. Typically, fluorescence emission spectra of the ITR probe (10 μM) in the absence and presence of 5 equiv. of various reference metal ions, Na^{+}, K^{+}, Li^{+}, Co^{2+}, Mg^{2+}, Cr^{3+}, Ni^{2+}, Cu^{2+}, Zn^{2+}, Pb^{2+}, Ag^{+},

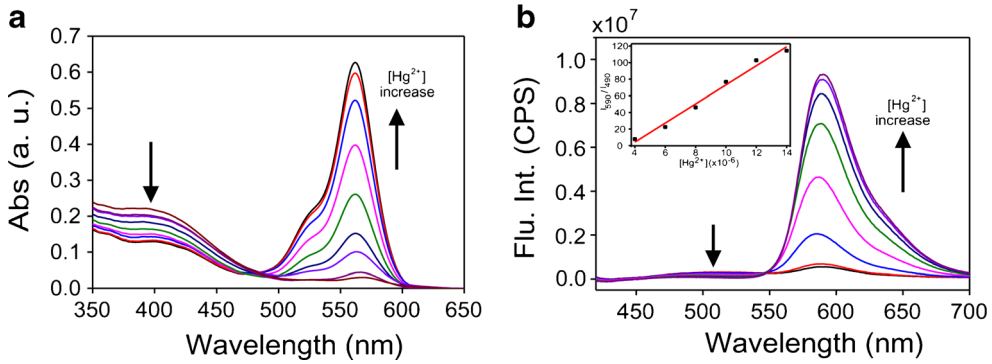

Fig. 3 Absorption spectra (**a**) and fluorescence emission spectra (λ_{ex}=390 nm) (**b**) of the probe in EtOH-MOPS mixed solvent with 70 % MOPS upon gradual addition of Hg^{2+} (0.0, 0.2, 0.4, 0.6, 0.8, 1.0, 1.2, 1.4, 1.6 equiv.)

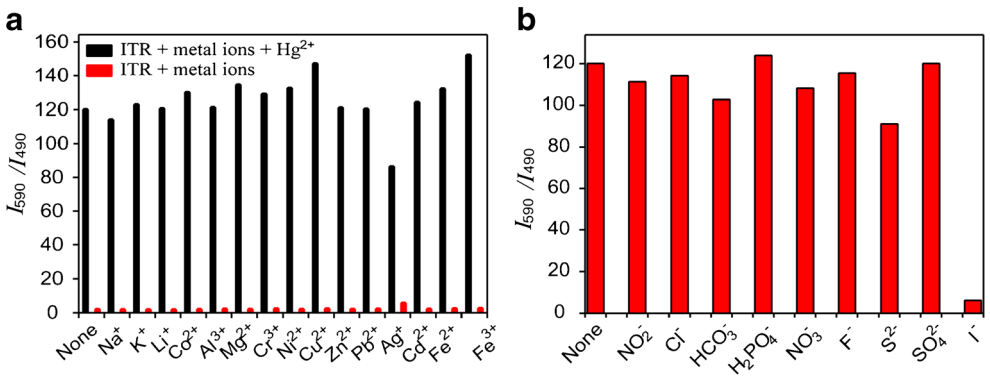

Fig. 4 Fluorescence intensity ratio (I_{590}/I_{490}) (λ_{ex}=390 nm) of probe (10 μM) in EtOH-MOPS mixed solvent with 70 % MOPS after addition of Hg^{2+} (20 μM) in the presence of other metal ions (50 μM) (**a**) and common anions (50 μM) (**b**)

Cd^{2+}, Fe^{2+}, and Fe^{3+}, respectively, were acquired firstly and then the counterpart spectrum of each sample with subsequent addition of 2 equiv. of Hg^{2+} were acquired under the identical condition. By calculating the I_{590}/I_{490} ratio of each spectrum and comparing the ratio values in each pair of probe sample, namely samples before and after the addition of Hg^{2+}, the binding features of probe to Hg^{2+} in the presence of various interfering metal ions were obtained, as shown in Fig. 4a. It can be clearly seen that the coexistence of most interfering metal ions can hardly interfere the binding of Hg^{2+} to the probe, definitely indicating the ion selectivity of the ITR probe for Hg^{2+} against other metal ions. It can be seen that the coexistence of Ag^{+} likely exerted discernable influence on the binding of Hg^{2+} to the probe, likely due to the prior coordination of Ag^{+} with the S atom of rhodamine and N atom of trizole. However, in such case, the I_{590}/I_{490} ratio after the addition of Hg^{2+} was 15 times larger than that of the sample prior to the addition of Hg^{2+}, even if the concentration of Ag^{+} was 2.5 times that of the Hg^{2+}. Unequivocally, such contrast is high enough for a reliable discrimination of Hg^{2+} from Ag^{+}. Figure 4b illustrates the influence of anions on Hg^{2+}-induced fluorescence increasing of the ITR probe. Taking that the fluorescence intensity of the probe solution almost kept unchanged upon addition of Na^{+}, as demonstrated in Fig. 4a, inorganic sodium salts containing typical anions such as NO_2^-, Cl^-, HCO_3^-, $H_2PO_4^-$, NO_3^-, F^-, S^{2-}, SO_4^{2-}, I^- were used as the sources of anions in the experiment. It can be seen from that the presence of these typical anions did not exert remarkable on the fluorescence intensity ratio I_{590}/I_{490} of the probe upon addition of Hg^{2+} except iodine anion. Owing to the poor solubility of HgI_2 salt in water, I^- actually functioned as the Hg^{2+} chelator for the sequestration of Hg^{2+} and therefore significantly supressed the Hg^{2+}-assisted ring-opening reaction of the ring-closed rhodamine moiety. As a result, the remarkably decreased fluorescence intensity ratio I_{590}/I_{490} of the probe in the presence of I^- upon addition of Hg^{2+}, as compared to the cases in the presence of other types of anions, was observed.

Figure 5 displays the recoverability of the fluorescence emission spectrum of the ITR probe upon alternating binding and debinding of Hg^{2+}. Specifically, taking the negligible influence that K^{+} exerted on the fluorescence emission features of the probe, KI was used as the Hg^{2+} chelator for sequestration of Hg^{2+}. It can be seen that the fluorescence emission band centered at 590 nm significantly increased upon addition of 1 equiv. of Hg^{2+} and such fluorescence enhancement was completely offset by the subesequent addition of 5 equiv. of KI, suggesting the perfect recoverability of the fluorescence emission features of the as-prepared hybrid NPs in the present

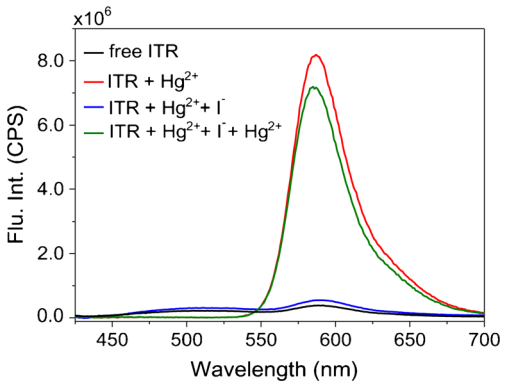

Fig. 5 Fluorescence emission spectrum of the free probe sample (*black curve*), that of the probe sample upon addition of 1 equiv. of Hg^{2+} (*red curve*), that of the probe sample after the sequential addition of 1 equiv. of Hg^{2+} and 5 equiv. of KI (*blue curve*) and that of the probe sample upon sequential addition of 1 equiv. of Hg^{2+}, 5 equiv. of KI, and another 5 equiv. of Hg^{2+} (*green curve*)

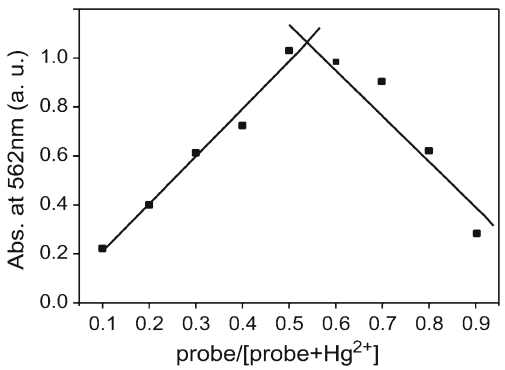

Fig. 6 Job's plot of changes in the absorbance (at 562 nm) of the probe sample at varying mole ratio of probe and Hg^{2+}, [probe]+[Hg^{2+}]=20 μM in EtOH-MOPS mixed solvent with 70 % MOPS

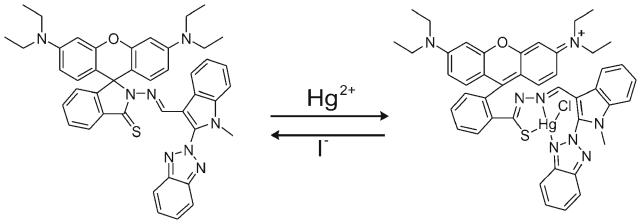

Scheme 2 Proposed reversible 1:1 binding mode between probe (IRT) and Hg^{2+}

work. It is noted that upon the subsequent addition of 5 equiv. of Hg^{2+}, fluorescence intensity of the probe sample after a increase-then-restoration cycle significantly increased again but displayed some discrepancy as compared to the intensity with Hg^{2+}-induced enhancement in the first round. The scattering factor due to the formation of HgI_2 precipitate in the aqueous sample, as well as the possible entrapment of the ITR molecules in the HgI_2 precipitate most probably affected the fluorescence recoverability of the sample and therefore contributed to such discrepancy.

Job's plot analysis was investigated to obtain the information about Hg^{2+}-probe complexation in EtOH-MOPS mixed solvent with 70 % MOPS (v/v). As shown in Fig. 6, the Job's plot analysis result obtained using continuous variation with a total concentration of 20 μM probe and Hg^{2+} exhibited a maximum absorbance value at ~0.5 mol fraction of Hg^{2+}, indicating the formation of a 1:1 stoichiometric complex of probe-Hg^{2+}. Such speculation about the formation of a 1:1 stoichiometric complex found support from the MALDI-TOF MS characterization results of the ITR probe sample prior to and after the addition of $HgCl_2$. Specifically, the free probe displayed a characteristic mass-to-charge ratio at m/z= 729.5 (Calcd. 730.3) while the ITR-Hg^{2+} complex presented a characteristic mass-to-charge ratio at m/z=967.5 that matches the structure of Hg^{2+}-Cl-ITR. Thus, the Job's plot analysis result and the MALDI-TOF MS characterization results verified the 1:1 stoichiometry of the complex, with the possible binding/debinding mechanism shown in Scheme 2.

The effects of pH on the fluorescence emission features of the probe were also investigated. Figure 7a displayed the fluorescence intensity ratio, I_{590}/I_{490}, of IRT probe in mixed solvent with various pH value in the absence and presence of Hg^{2+}. It can be clearly seen that the I_{590}/I_{490} ratio of the free probe sample did not displayed discernable change upon changing the pH value in the range of pH 1.0–11.0, suggesting the excellent stability of the probe even in such broad range of acidic/alkaline milieu. Importantly, the probe sample under the pH region of 7.2–7.4 in the presence of Hg^{2+} exhibited the maximum I_{590}/I_{490} ratio up to 137, in sharp contrast to the counterpart ratio of the free probe, indicating the most sensitive response feature of the ITR probe to Hg^{2+} in the typical physiological pH conditions. Figure 7b displayed time-dependent fluorescence intensity ratio (I_{590}/I_{490}) of probe in EtOH-MOPS mixed solvent in the presence of Hg^{2+}. It can be clearly seen that the fluorescence signal of the probe reached a saturated state approximately 5 min after the addition of Hg^{2+} and faithfully kept stable thereafter, suggesting the prompt stimuli-response features and stable signal output of the IRT probe for Hg^{2+} sensing. Taking this, along with the aforementioned maximum fluorescence signal in the typical physiological pH conditions, such new type of probe ia expected to have great potential for practical Hg^{2+} sensing.

The applicability of the probe for intracellular Hg^{2+} sensing was also confirmed with the results shown in Fig. 8. In a typical imaging experiment, MCF-7 cells were incubated with 10 μM IRT probe in DMEM medium at 37 °C for 30 min before the acquisition of the DIC (Fig. 8a) and fluorescence images of the cells via confocal laser scanning microscopy (CLSM). It can be seen that the cells with internalized ITR probes exhibited faint fluorescence (Fig. 8b). Subsequently, the cells were treated with Hg^{2+} (10 μM) for another 30 min at 37 °C and then the fluorescence images of the cells with internalized ITR probes and Hg^{2+} were acquired. In sharp contrast to the faint fluorescence of the cells before the treatment of Hg^{2+}, the fluorescence images of the cells after the treatment of Hg^{2+} acquired exhibited cellular contours with much stronger brightness, a result of the Hg^{2+}-induced fluorescence enhancement in the red fluorescence region (Fig. 8c). Such a dramatic contrast in fluorescence brightness between Fig. 8b and c clearly demonstrated the usefulness of the as-prepared ITR probe for intracellular Hg^{2+} sensing.

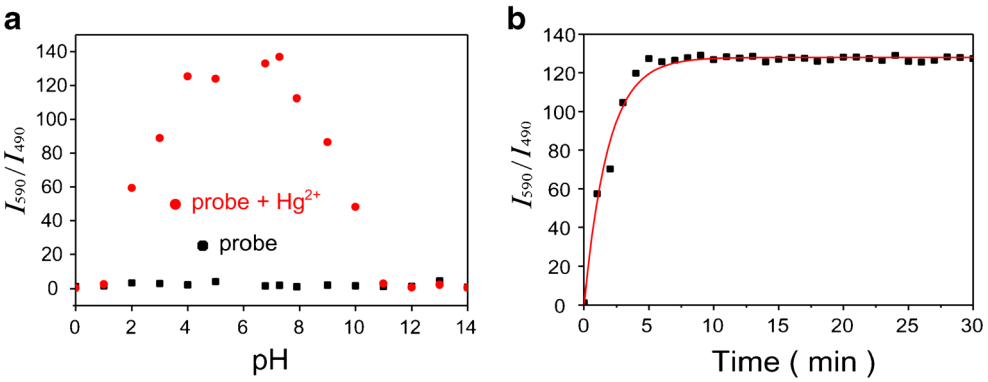

Fig. 7 The PH- (**a**) and time-dependent (**b**) fluorescence intensity ratio (I_{590}/I_{490}) (λ_{ex}= 390 nm) of the probe in EtOH-MOPS mixed solvent with 70 % MOPS upon addition of 2 equiv. of Hg^{2+}

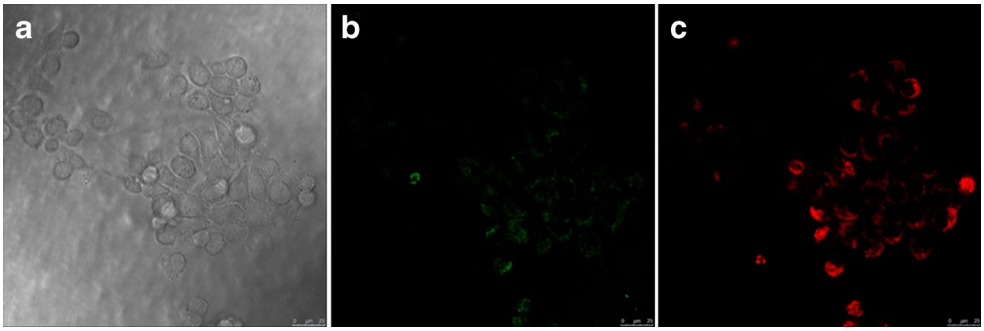

Fig. 8 The bright field (**a**) and CLSM fluorescence images (**b**) of the MCF-7 cells with internalized ITR probe; the CLSM fluorescence images of the MCF-7 cells shown in (**a**) and (**b**) after the following incubation with Hg^{2+}

Conclusion

In summary, we have developed a new type of indole-trizole-rhodamine triad based ratiometric fluorescent probe for Hg^{2+} sensing. The as-prepared fluorescent probe is capable of detecting Hg^{2+} over other reference metal ions including Ag^{+} with high selectivity. The indole-trizole conjugate provides coordination site for Hg^{2+} recognition and meanwhile functions as the energy donor while the rhodamine hydrazide moiety undergoes Hg^{2+}-assisted ring-opening reaction yielding ring-open rhodamine product acting as the energy acceptor. The synergistic effect of the huge contrast in the fluorescence signal that the ring-open and ring-closed moiety bestowed and the FRET-enabled amplification in the fluorescence signal of the probe contributed to a detection limit of 11 nm for Hg^{2+} sensing. Additionally, the Hg^{2+}-induced marked change in the color of the probe solution bestowed this type of probes with practicability for facile visual detection of Hg^{2+} by human eyes. The preliminary cell experiment results have revealed the practicability of this type of probes for intracellular Hg^{2+} sensing.

Acknowledgments Financial support from the National Natural Science Foundation of China (grant no. 21173262 and 21373218) and the "Hundred-Talent Program" of CAS to ZT is acknowledged.

References

1. Tan SW, Meiller JC, Mahaffey KR (2009) The endocrine effects of mercury in humans and wildlife. Crit Rev Toxicol 39(3):228–269
2. Clarkson TW, Magos L (2006) The toxicology of mercury and its chemical compounds. Crit Rev Toxicol 36(8):609–662
3. Gutknecht J (1981) Inorganic mercury (Hg^{2+}) transport through lipid bilayer membranes. J Membr Biol 61(1):61–66
4. Carvalho CML, Chew E-H, Hashemy SI, Lu J, Holmgren A (2008) Inhibition of the human thioredoxin system: a molecular mechanism of mercury toxicity. J Biol Chem 283(18):11913–11923
5. Clarkson TW, Magos L, Myers GJ (2003) The toxicology of mercury-current exposures and clinical manifestations. N Engl J Med 349(18):1731–1737
6. Mahato P, Saha S, Das P, Agarwalla H, Das A (2014) An overview of the recent developments on Hg^{2+} recognition. RSC Adv 4(68): 36140–36174
7. Kumar N, Bhalla V, Kumar M (2014) Resonance energy transfer-based fluorescent probes for Hg^{2+}, Cu^{2+} and Fe^{2+}/Fe^{3+} ions. Analyst 139(3):543–558
8. Kim HN, Ren WX, Kim JS, Yoon J (2012) Fluorescent and colorimetric sensors for detection of lead, cadmium, and mercury ions. Chem Soc Rev 41(8):3210–3244
9. Gao Y, De Galan S, De Brauwere A, Baeyens W, Leermakers M (2010) Mercury speciation in hair by headspace injection–gas chromatography–atomic fluorescence spectrometry (methylmercury) and combustion-atomic absorption spectrometry (total Hg). Talanta 82(5):1919–1923
10. Resano M, Aramendia M, Rello L, Calvo ML, Berail S, Pecheyran C (2013) Direct determination of Cu isotope ratios in dried urine spots by means of fs-LA-MC-ICPMS. Potential to diagnose Wilson's disease. J Anal Atom Spectrom 28(1):98–106
11. Chen Y-W, Tong J, D'Ulivo A, Belzile N (2002) Determination of mercury by continuous flow cold vapor atomic fluorescence spectrometry using micromolar concentration of sodium tetrahydroborate as reductant solution. Analyst 127(11):1541–1546
12. Sareen D, Kaur P, Singh K (2014) Strategies in detection of metal ions using dyes. Coord Chem Rev 265:125–154
13. Santos-Figueroa LE, Moragues ME, Climent E, Agostini A, Martinez-Manez R, Sancenon F (2013) Chromogenic and fluorogenic chemosensors and reagents for anions. A comprehensive review of the years 2010-2011. Chem Soc Rev 42(8):3489–3613
14. Vendrell M, Zhai D, Er JC, Chang Y-T (2012) Combinatorial strategies in fluorescent probe development. Chem Rev 112(8):4391–4420
15. Zhang JF, Zhou Y, Yoon J, Kim JS (2011) Recent progress in fluorescent and colorimetric chemosensors for detection of precious metal ions (silver, gold and platinum ions). Chem Soc Rev 40(7): 3416–3429
16. Ozturk S, Atilgan S (2014) A tetraphenylethene based polarity dependent turn-on fluorescence strategy for selective and sensitive detection of Hg2+ in aqueous medium and in living cells. Tetrahedron Lett 55(1):70–73
17. Fu N, Chen Y, Fan J, Wang G, Lin S (2014) A bifunctional "Turn On" fluorescent probe for trace level Hg^{2+} and EDTA in aqueous solution via chelator promoted cation induced deaggregation signalling. Sensors Actuators B Chem 203:435–443
18. Ma X, Wang J, Shan Q, Tan Z, Wei G, Wei D, Du Y (2012) A "turn-on" fluorescent Hg^{2+} chemosensor based on Ferrier carbocyclization. Org Lett 14(3):820–823
19. Yang Y-K, Yook K-J, Tae J (2005) A rhodamine-based fluorescent and colorimetric chemodosimeter for the rapid detection of Hg^{2+} ions in aqueous media. J Am Chem Soc 127(48):16760–16761
20. Lv Y, Zhu L, Liu H, Wu Y, Chen Z, Fu H, Tian Z (2014) Single-fluorophore-based fluorescent probes enable dual-channel detection of Ag^{+} and Hg^{2+} with high selectivity and sensitivity. Anal Chim Acta 839:74–82

21. Pandey S, Azam A, Pandey S, Chawla HM (2009) Novel dansyl-appended calix[4]arene frameworks: fluorescence properties and mercury sensing. Org Biomol Chem 7(2):269–279
22. Moon S-Y, Youn NJ, Park SM, Chang S-K (2005) Diametrically disubstituted cyclam derivative having Hg^{2+}-selective fluoroionophoric behaviors. J Org Chem 70(6):2394–2397
23. Métivier R, Leray I, Valeur B (2004) Lead and mercury sensing by calixarene-based fluoroionophores bearing two or four dansyl fluorophores. Chem Eur J 10(18):4480–4490
24. Tsien RY, Poenie M (1986) Fluorescence ratio imaging: a new window into intracellular ionic signaling. Trends Biochem Sci 11(11):450–455
25. Yuan L, Lin W, Zheng K, Zhu S (2013) FRET-based small-molecule fluorescent probes: rational design and bioimaging applications. Acc Chem Res 46(7):1462–1473
26. Fan J, Hu M, Zhan P, Peng X (2013) Energy transfer cassettes based on organic fluorophores: construction and applications in ratiometric sensing. Chem Soc Rev 42(1):29–43
27. Chen G, Song F, Xiong X, Peng X (2013) Fluorescent nanosensors based on fluorescence resonance energy transfer (FRET). Ind Eng Chem Res 52(33):11228–11245
28. Chen X, Pradhan T, Wang F, Kim JS, Yoon J (2011) Fluorescent chemosensors based on spiroring-opening of xanthenes and related derivatives. Chem Rev 112(3):1910–1956
29. Zhang T, Chan C-F, Lan R, Wong W-K, Wong K-L (2014) Highly selective and responsive visible to near-IR Ytterbium emissive probe for monitoring mercury(II). Chem Eur J 20(4):970–973
30. Wang C, Zhang D, Huang X, Ding P, Wang Z, Zhao Y, Ye Y (2014) A ratiometric fluorescent chemosensor for Hg^{2+} based on FRET and its application in living cells. Sensors Actuators B Chem 198: 33–40
31. Li K-B, Zhang H-L, Zhu B, He X-P, Xie J, Chen G-R (2014) A peracetyl glycosyl rhodamine as a novel fluorescent ratiometric probe for mercury (II). Dyes Pigments 102:273–277
32. Luxami V, Verma M, Rani R, Paul K, Kumar S (2012) FRET-based ratiometric detection of Hg^{2+} and biothiols using naphthalimide-rhodamine dyads. Org Biomol Chem 10(40):8076–8081
33. Ma Q-J, Zhang X-B, Zhao X-H, Jin Z, Mao G-J, Shen G-L, Yu R-Q (2010) A highly selective fluorescent probe for Hg^{2+} based on a rhodamine–coumarin conjugate. Anal Chim Acta 663(1):85–90
34. Zhang X, Xiao Y, Qian X (2008) A ratiometric fluorescent probe based on FRET for imaging Hg^{2+} ions in living cells. Angew Chem Int Ed 47(42):8025–8029
35. Wen J, Zhu L-L, Bi Q-W, Shen Z-Q, Li X-X, Li X, Wang Z, Chen Z (2014) Highly N2-selective coupling of 1,2,3-triazoles with indole and pyrrole. Chem Eur J 20(4):974–978
36. Rurack K, Kollmannsberger M, Resch-Genger U, Daub J (2000) A selective and sensitive fluoroionophore for Hg(II), Ag(I), and Cu(II) with virtually decoupled fluorophore and receptor units. J Am Chem Soc 122:968
37. Liu L, Zhang GX, Xiang JF, Zhang DQ, Zhu DB (2008) Fluorescence "turn on" chemosensors for Ag^{+} and Hg^{2+} based on tetraphenylethylene motif featuring adenine and thymine moieties. Org Lett 10:4581
38. Chen T, Zhu WP, Xu YF, Zhang SY, Zhang XJ, Qian XH (2010) Discovery of a highly selective turn-on fluorescent probe for Ag^{+}. Dalton Trans 39:1316
39. Xu ZC, Zheng SJ, Yoon JY, Spring DR (2010) Discovery of a highly selective turn-on fluorescent probe for Ag^{+}. Analyst 135: 2554
40. Kai Y, Yang S, Gao X, Hu Y (2014) Colorimtric and "turn-on" fluorescent for Hg^{2+} based on rhodamine-3,4-ethylenedioxythiophene derivative. Sensors Actuators B Chem 202:252–256